

Selenadiazole-Induced Hela Cell Apoptosis through the Redox Oxygen Species-Mediated JAK2/STAT3 Signaling Pathway

Yi Yuan,[†] Yinghua Li,[†] Qinglin Deng, Jinying Yang,* and Jing Zhang*Cite This: *ACS Omega* 2024, 9, 20919–20926

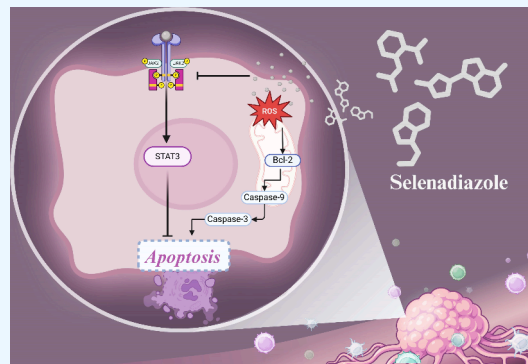
Read Online

ACCESS |

Metrics & More

Article Recommendations

ABSTRACT: Cervical cancer is a significant global health concern, and novel therapeutic strategies are continually being sought to combat this disease. In recent years, selenadiazole found latent therapeutic effects on tumors. Herein, investigating the mechanism of selenadiazole in Hela cells holds promise for advancing cervical cancer treatment. Hela cells, a widely utilized model for studying cervical cancer, were treated with selenadiazole, and cell viability was assessed by using the cell counting kit-8 (CCK-8) assay. Changes in mitochondrial membrane potential were evaluated using JC-1 staining, while apoptosis induction was examined using AnnexinV–PI double staining. Intracellular ROS levels were measured by using specific fluorescent probes and the ELIASA system. Additionally, Western blotting was performed to assess the activation of related proteins in response to selenadiazole. Data analysis was performed using GraphPad. Exposure to selenadiazole led to a substantial increase in intracellular redox oxygen species (ROS) levels in Hela cells. Importantly, the induction of ROS by selenadiazole was associated with a marked increase in mitochondrial apoptosis, as evidenced by elevated levels of AnnexinV-positive cells, the JC-1 monomer, caspase-9, and Bcl-2. Furthermore, activation of the JAK2/STAT3 pathway was observed following the selenadiazole treatment. Selenadiazole holds the potential to suppress tumor growth in cervical cancer cells by increasing reactive oxygen species (ROS) levels and inducing mitochondrial apoptosis via the JAK2/STAT3 pathway. This study offers valuable insights into potential cervical cancer therapies and underscores the need for further research into the specific mechanisms of selenadiazole.



INTRODUCTION

Cervical cancer remains a pressing and life-threatening issue, affecting women worldwide with a high morbidity rate of 13.3 per 100,000 in 2020.¹ Tragically, it stands as the most frequent cause of death among women in developing countries.² What is even more concerning is the observation that the average age of onset for cervical cancer has seen a concerning decline of 5–10 years compared to the past decade. This alarming trend emphasizes the urgent need for effective interventions and treatments. Despite remarkable progress in the development of vaccines targeting high-risk human papillomavirus (HR-HPV) and the advancement of radiotherapy and chemotherapy, there remains a striking surplus of patients who face rapid disease progression or recurrence or even find themselves in an incurable situation. This can be attributed to several factors, including potential HR-HPV infections and the inherent heterogeneity of cervical cancer. It is crucial to acknowledge that, while HR-HPV vaccination efforts have been accelerated,³ a significant proportion of patients still experience challenges due to the diverse nature of HR-HPV strains and their impact on disease progression. Additionally, the complex and heterogeneous nature of cervical cancer itself poses obstacles in effectively treating and managing the condition.⁴ These factors contribute to the persistence and overabundance of

patients facing unfavorable outcomes. Addressing these challenges requires a comprehensive approach that encompasses improved screening strategies, targeted therapies, and a deeper understanding of the intricate mechanisms driving the progression and recurrence of cervical cancer. By investing in research and innovation, we can strive to reduce the burden of this devastating disease and improve outcomes for patients worldwide.

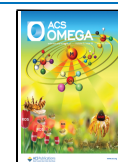
ROS plays a crucial role in the intricate web of intrinsic biochemical processes, showcasing their unique and multifaceted impact on both organism growth and programmed cell death.⁵ On one hand, ROS can instigate DNA damage when there is an imbalance between pro-oxidants and antioxidants, potentially triggering genomic alterations and even cell death.⁶ However, it is important to note that ROS also assumes a significant role in the realm of cancer progression and

Received: December 18, 2023

Revised: March 21, 2024

Accepted: April 17, 2024

Published: April 30, 2024



development.⁶ It actively influences cancerous behavior by signaling cell death pathways and shaping the immune microenvironment.⁷ This interplay between ROS and biochemical effects has propelled research efforts toward ROS-modulating therapies, which have emerged as a compelling and pivotal focus for suppressing tumorigenesis. By harnessing the intricate relationship between ROS and cellular processes, we strive to unlock new avenues for combating cancer and enhancing therapeutic outcomes.

Selenium (Se) is a micronutrient acting as an inflammation, oxidant, and tumor suppressor in humans.^{8,9} The paucity of selenium throughout the metabolism is bound up with Keshan disease, malignant tumors, and infertility.^{10–12} Notably, prior studies have highlighted its extraordinary effects in abrogating hepatocellular carcinoma, colon cancer, prostate cancer, lung cancer, and even H1N1 virus infection through ROS-induced apoptosis.^{13,14} Selenadiazole, a synthetic agent, exerts an antiproliferation function in human breast adenocarcinoma MCF-7 cells and is also a radiosensitizer in melanoma A375 cell.^{15,16} In MCF-7, selenadiazole elicits an overabundance of oxidants and DNA fragmentation, thus activating caspase, Bcl-2, and other pro-apoptosis proteins. Simultaneously, selenadiazole enhances the sensitivity of radiotherapy by eliciting G2/M cell cycle arrest and ascending the ROS level, which synergistically hinders cancerous activity.

It is important to highlight that, while the potential of selenadiazole in inhibiting pan-cancer activity is complex, its specific therapeutic mechanism in various cancers remains unresolved. In this study, we aim to investigate the anticancer effects of selenadiazole in cervical cancer HeLa cells and elucidate its underlying molecular mechanisms. Our findings are anticipated to offer insights into a practical chemotherapeutic approach for cervical cancer, potentially contributing significantly to our understanding of the pathogenesis of this disease.

RESULTS AND DISCUSSION

Selenadiazole Inhibited the Viability of HeLa Cells.

Figure 1A demonstrates that cell viability gradually descended as the concentration of selenadiazole increased (0, 10, 20, 25, and 30 μM), implying a dose–response relationship. In Figure 1B, we further confirmed the inhibition potential of selenadiazole. Compared with the control group, the inhibition ratio of the 25 μM group and 30 μM group showed apparent differences with $P < 0.01$ and $P < 0.001$, respectively. Notwithstanding an apparent trend of cell viability, no significant difference was detected between the control group and either the 10 μM group or 20 μM group ($P > 0.05$).

Consistent with prior studies, our findings demonstrated that selenadiazole inhibited cell viability.^{16,17} The selection of appropriate dosages was performed by using CCK-8. Selenadiazole exerted cytotoxic effects on HeLa cells. Beginning with 10 μM , the increasing dosages of selenadiazole were synchronized with descending cell viability (Figure 1). To better investigate the intrinsic mechanism of selenadiazole, we utilized the concentrations of 10, 20, and 30 μM in the following experiment. To elucidate the anticancerous effects of selenadiazole, we applied wound-healing assay and apoptosis-related experiments subsequently.

Selenadiazole Inhibited Cell Migration of HeLa Cells.

Furthermore, to explore the latent functions of selenadiazole in suppressing tumor genesis, we conducted a wound-healing assay. The results of the wound-healing assay under different

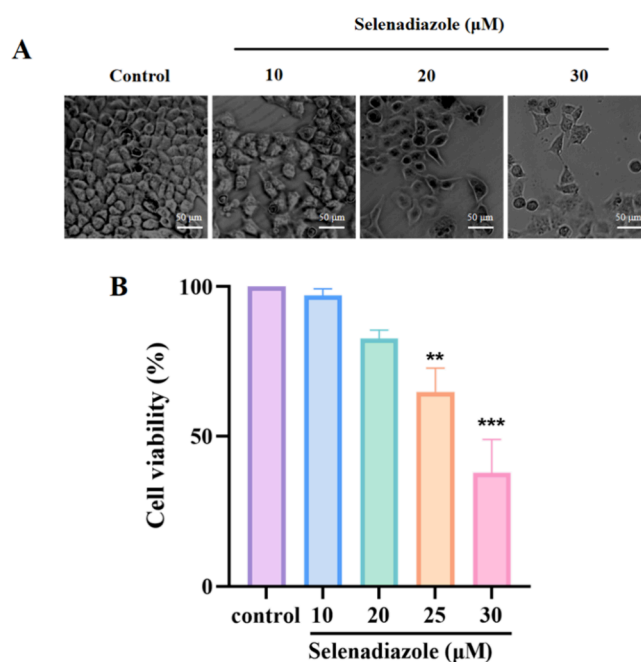


Figure 1. Effects of selenadiazole in cell viability. (A) Morphological features of HeLa cells under different doses of selenadiazole. (B) Cell viability under different doses of selenadiazole was detected by CCK-8 compared with the control group. * denotes $P < 0.05$, ** denotes $P < 0.01$, and *** denotes $P < 0.001$.

doses of selenadiazole in Figure 2A indicated that selenadiazole exerted a role as a migration inhibitor in HeLa cells. After measurement of the scratch widths, we found that the wound-healing rates of the 10, 20, and 30 μM group were significantly increased ($P < 0.05$) compared with the control group (Figure 2B).

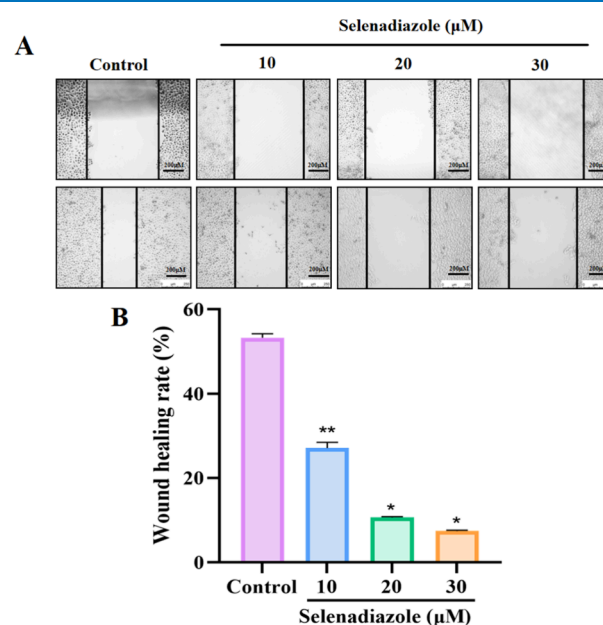


Figure 2. Effects of selenadiazole in cell migration. (A) Results of the wound-healing assay under different doses of selenadiazole. (B) Results of the wound-healing rate under different doses of selenadiazole compared with the control group. * denotes $P < 0.05$, ** denotes $P < 0.01$, and *** denotes $P < 0.001$.

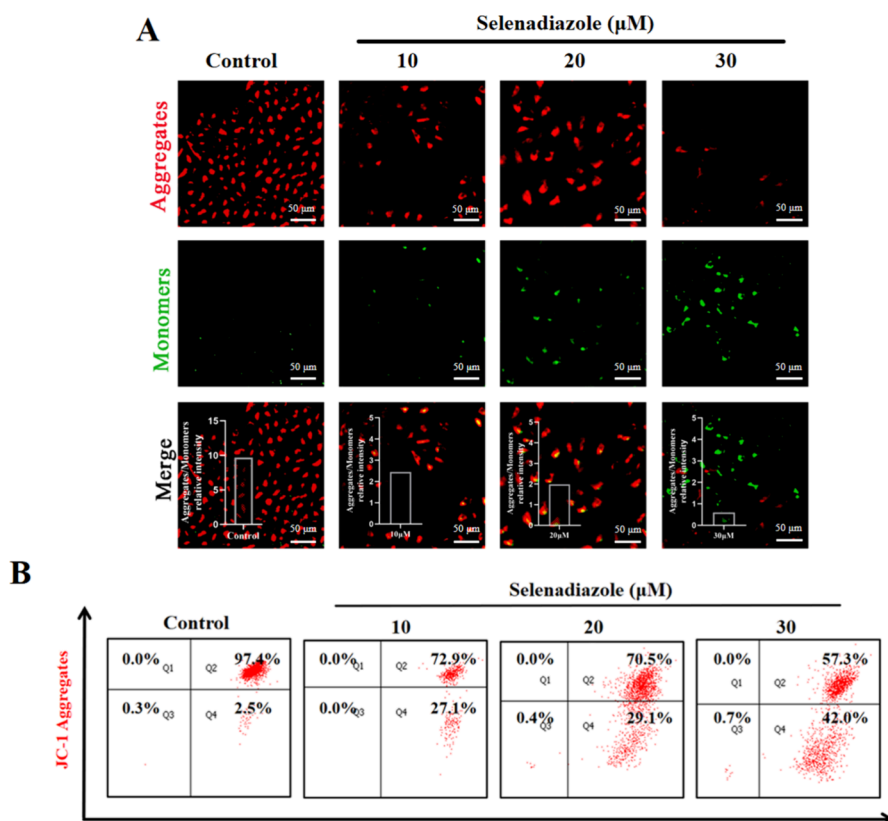


Figure 3. Selenadiazole affects mitochondrial membrane potential ($\Delta\Psi\text{m}$). (A) JC-1 aggregates and monomers of HeLa cells under different doses of selenadiazole. (B) Flow cytometry results of JC-1 aggregates and monomers under different doses of selenadiazole.

Cell migration is a crucial ability for cancerous cells to remodel vessels and forth deteriorate tumor genesis in cervical cancer.¹⁸ Paralleled with results of cell viability, Figure 2 depicts that wound-healing rates of the 10, 20, and 30 groups were significantly increased compared with the control group. Notably, wound-healing assay is a two-dimension cell migration assay, which could provide a snapshot of cell capacity,¹⁹ and a concrete mechanism of migration phenotype should be further investigated.

Selenadiazole Affects Mitochondrial Membrane Potential ($\Delta\Psi\text{m}$). The decreasing of mitochondrial membrane potential ($\Delta\Psi\text{m}$) is one of the tokens of early stage apoptosis.²⁰ Here, selenide triggered mitochondria depolarization, thus resulting in intracellular dysfunction. As depicted in Figure 3A, fluorescence staining showed that selenadiazole decreased the levels of JC-1 aggregates but increased the levels of JC-1 monomers in HeLa cells as the concentrations of selenadiazole ascended, which indicated that selenadiazole enabled the descending of mitochondrial membrane potential. We also quantized the JC-1 changes by calculating the intensity ratio between green fluorescence and red fluorescence in Figure 3A. Then, we digested the HeLa cells and applied JC-1 staining to quantitatively identify the mitochondrial membrane potential ($\Delta\Psi\text{m}$) through flow cytometry. Figure 3B demonstrates that the JC-1 aggregates descended shown in the Q2 quadrant, while JC-1 monomers ascended shown in the Q4 quadrant with percentages of 2.5, 27.1, 29.1, and 42.0%, following the addition of selenadiazole.

Mitochondria participate in a large amount of cellular function, including ATP generation, glycometabolism, lipid metabolism, and oxidants-antioxidants balance.²¹ Presently, we

found that selenadiazole damaged the mitochondrial membrane by using the JC-1 assay (Figure 3). More JC-1 monomers were detected following the increasing levels of selenadiazole, indicating the descending mitochondrial membrane potential. The alterations of morphological features in mitochondria may subsequently induce the imbalance between oxidants and antioxidants,²² which requires further experimental proof.

Selenadiazole-Induced Apoptosis in HeLa Cells. When apoptosis occurred, the inner layer of the phospholipid bilayer everted. In that capacity, AnnexinV staining reagents enabled binding to serine inside the inner layer. PI staining reagents were capable of gaining access into necrotic or late-stage apoptosis cells and emitted red fluorescence. Here, we found that selenadiazole induced early and late-stage apoptosis (Figure 4A). We have used red, green, and black arrows to assign the apoptotic, necrotic, and living cells, respectively. Of note, a swollen and dense nucleus is the token to identify the apoptotic cell. Then, the necrotic cell is recognized by its incomplete cytomembrane and intracellular vacuoles. Our flow cytometry analysis also indicated that selenadiazole gradually induced cell apoptosis with elevated percentages of 1.6, 2.9, 4.7, and 5.1% in early stage apoptosis and 1.1, 2.6, 3.9, and 5.7% in late-stage apoptosis.

The damage to the mitochondria membrane inhibits the Bcl-2 family and activates caspase-9, thus triggering mitochondrial apoptosis.^{23,24} Apoptosis is characterized by an everted phospholipid bilayer, which can be detected by AnnexinV staining. Our results of AnnexinV-PI double staining demonstrated selenadiazole-induced apoptosis. Lumped up with previous results of elevated JC-1 monomers, we could

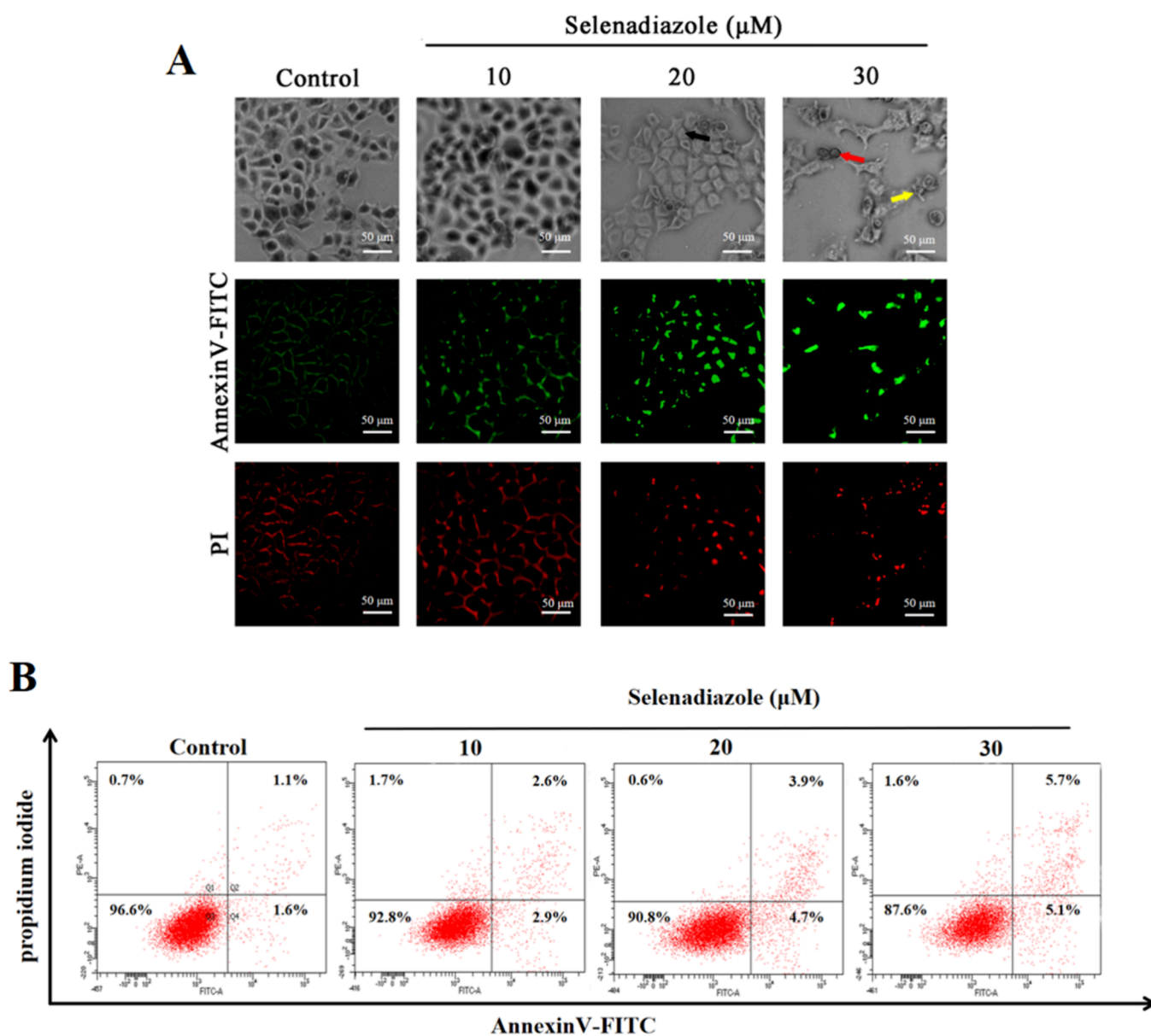


Figure 4. Selenadiazole induced apoptosis in Hela cells. (A) AnnexinV and PI in Hela cells under different doses of selenadiazole. (B) Flow cytometry results of AnnexinV and PI under different doses of selenadiazole. The red, green, and black arrows assign the apoptotic, necrotic, and living cells, respectively.

conclude that selenadiazole possibly triggered mitochondrial apoptosis. Of note, it is noteworthy whether selenadiazole-induced mitochondrial apoptosis should be further confirmed through the detection of the caspase-9 and Bcl-2 family.

Selenadiazole-Induced Apoptosis through the Intrinsic Pathway. In intrinsic apoptosis, the homeostasis of the Bcl-2 family started to disappear as DNA was damaged, thus resulting in the activation of caspase-9.²² Caspase-9 stimulated an apoptotic cascade reaction and triggered the cleaving of caspase-3 ultimately.²¹ Here, we found that selenadiazole-activated poly ADP-ribose polymerase (PARP), caspase-9, Bcl-2, and caspase-3 in Hela cells (Figure 5A). Bcl-2 levels ascended following the increasing doses of selenadiazole. Acted as a substrate of cleaved-caspase, the elevated expression of PARP was detected. The expression of caspase-9 started to augment ($P < 0.05$) as the concentration of selenadiazole elevated $P < 0.05$ (Figure 5B). Caspase-3 increased as the

concentration of selenadiazole elevated into 3 μM , with $P < 0.001$ (Figure 5B).

To elucidate the mechanism of selenadiazole-induced apoptosis, we detected the expressions of Bcl-2, caspase-3, caspase-9, and PARP. The levels of mitochondrial apoptosis-related proteins, Bcl-2, and caspase-9 decreased or increased following the increasing doses of selenadiazole, respectively (Figure 5). Additionally, the critical protein of apoptosis, caspase-3, increased as the concentration of selenadiazole rose.^{25,26} Collectively, we can clue that selenadiazole triggered impaired mitochondria and activated caspase-9-mediated mitochondrial apoptosis. It is worth noting that how selenadiazole causes caspase-9-mediated mitochondrial apoptosis remained unresolved. Considering the mitochondrial function and homeostasis of oxidants-antioxidants, ROS detection is needed to prove that selenadiazole could lead to ROS elevation, thus triggering mitochondrial apoptosis.

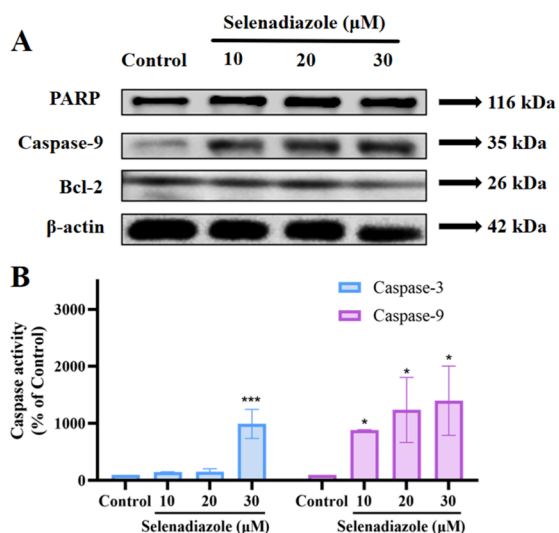


Figure 5. Expression of the apoptosis-related protein in HeLa cells under different doses of selenadiazole. (A) Western blotting analysis of PARP, caspase-9, and Bcl-2 in HeLa cells under different doses of selenadiazole. (B) Caspase activity under different doses of selenadiazole compared with the control group. * denotes $P < 0.05$, ** denotes $P < 0.01$, and *** denotes $P < 0.001$.

Selenadiazole-Induced ROS Generation. ROS is capable of activating a series of transcription factors and participating in apoptosis.^{27,28} DCFH cannot be detected by a fluorescence microscope only when DCFH is oxidated into DCF by intracellular ROS. In our study, we uncovered that the ROS levels gradually increased following the addition of selenadiazole (Figure 6A). Furthermore, we quantitatively detected ROS generation and found that ROS generation was significantly elevated with $P < 0.05$, $P < 0.0001$, and $P < 0.0001$, respectively (Figure 6B).

We applied DCFH to confirm ROS augmentation and validated that selenadiazole resulted in the aggregation of ROS

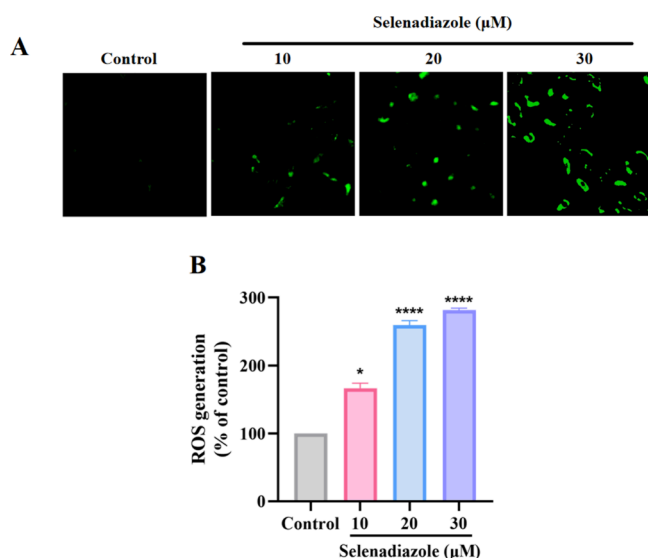


Figure 6. ROS overproduction induced by selenadiazole. (A) Changes in intracellular ROS under different doses of selenadiazole. (B) ROS generation under different doses of selenadiazole compared with the control group. * denotes $P < 0.05$, ** denotes $P < 0.01$, *** denotes $P < 0.001$, and **** denotes $P < 0.0001$.

(Figure 6). Until now, we have speculated that selenadiazole acts as a tumor suppressor via ROS-induced mitochondrial apoptosis in HeLa cells, whereas the intrinsic mechanism of selenadiazole in inducing ROS-mediated apoptosis remained unknown.

Selenadiazole-Activated JAK2/STAT3 Pathway. In Figure 7A, the elevated concentration of selenadiazole was synchronized with a decreased expression of JAK2, STAT3, and pSTAT3. Figure 7B–D demonstrates relative expression of JAK2, STAT3, and pSTAT3 among different doses of selenadiazole with statistical significance. These findings implied that selenadiazole triggered transcription factor STAT3 and activated the JAK2/STAT3 pathway. Lumped up the results mentioned above, we concluded that the JAK2/STAT3 pathway is presumably a cardinal signal pathway for selenadiazole in cell invasion and apoptosis.

Figure 7 shows that selenadiazole declined the expression of JAK2 and STAT3, which were documented as cell proliferating proteins.^{29–31} JAK2 is known to undergo activation upon binding of specific ligands to their respective cytokine receptors.³² This activation triggers the autophosphorylation of JAK proteins and subsequent phosphorylation of the associated receptors, thereby generating multiple binding sites for signal transduction proteins. Notably, the transcription factor, STAT3, is among the key molecules involved in these processes.³³ STAT3 has been demonstrated to exhibit persistent activation in various human tumors, and it possesses an oncogenic capacity along with antiapoptotic activity.³⁴ Together, our results implied that selenadiazole holds the potential for suppressing tumor growth in cervical cancer cells by increasing reactive oxygen species (ROS) levels and inducing mitochondrial apoptosis via the JAK2/STAT3 pathway.

The limitations of our study could not be ignored. First, the use of HeLa cells, while a well-established model for cervical cancer, may not fully represent the heterogeneity of cervical cancer. Future studies could benefit from validating the findings in other cell lines or primary cancer cells. Second, although our study provides valuable insights using *in vitro* models, translating these findings into an *in vivo* context is essential to assess the clinical significance and potential side effects of selenadiazole. Ultimately, the study highlights the activation of the JAK2/STAT3 pathway and ROS-induced apoptosis, additional experiments exploring the detailed molecular mechanisms underlying these processes would further strengthen the conclusions (Figure 8).

CONCLUSIONS

Selenadiazole holds the potential for suppressing tumor growth in cervical cancer cells by increasing reactive oxygen species (ROS) levels and inducing mitochondrial apoptosis via the JAK2/STAT3 pathway. This study offers valuable insights into potential cervical cancer therapies and underscores the need for further research into the specific mechanisms of selenadiazole.

METHODS AND MATERIALS

Cell Culture and Cell Viability Assay. HeLa cells, purchased from the American Type Culture Collection (ATCC, Manassas, VA, USA), were cultured in a humid incubator at 37 °C under a 5% CO₂ atm. The cells were grown in a complete medium, comprising Dulbecco's Modified Eagle

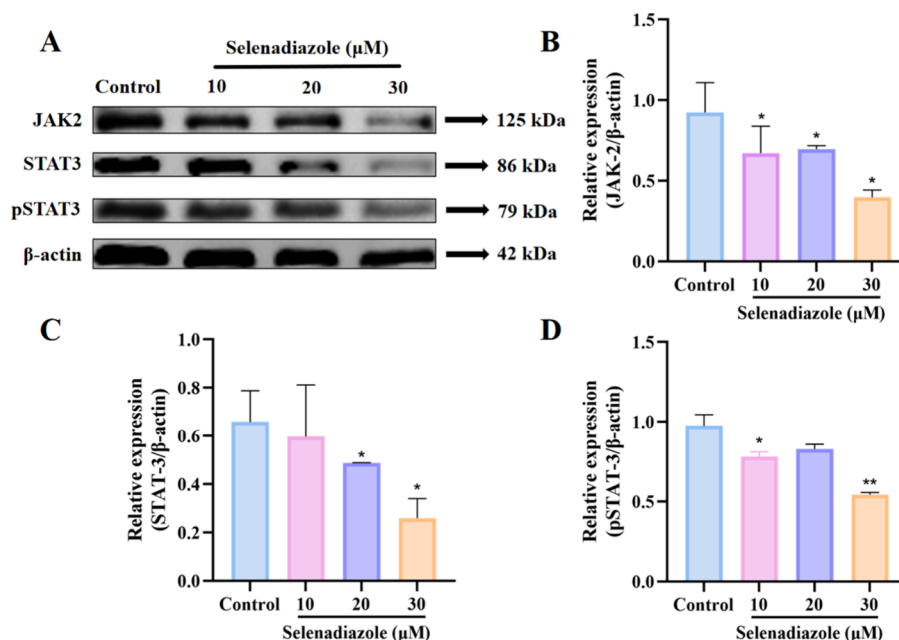


Figure 7. Selenadiazole triggered apoptosis through the JAK2/STAT3 pathway. (A) Western blotting analysis of HeLa cells exposed with different doses of selenadiazole. (B) Relative expression of JAK2 compared with β -actin. (C) Relative expression of STAT3 compared with β -actin. (D) Relative expression of pSTAT3 compared with β -actin. * denotes $P < 0.05$, ** denotes $P < 0.01$, and *** denotes $P < 0.001$.

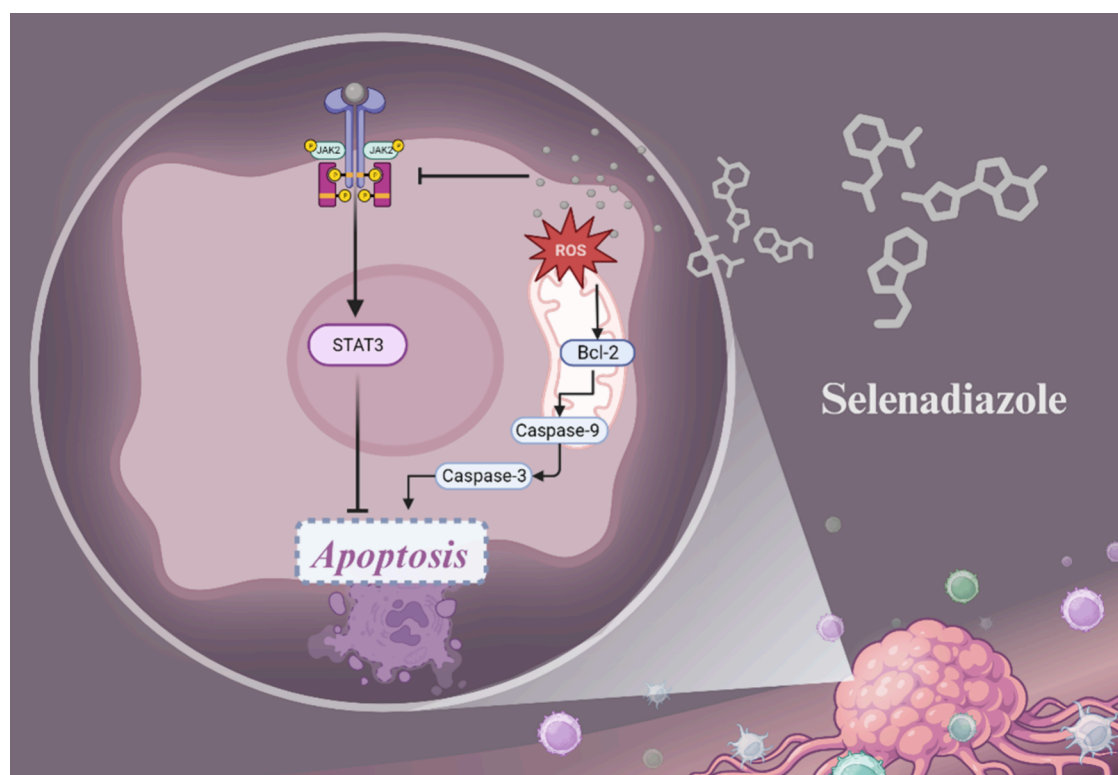


Figure 8. Schematic overview of selenadiazole's anticancerous capacities in HeLa cells. Selenadiazole induced mitochondrial apoptosis via the ROS-mediated JAK2/STAT3 signaling pathway.

Medium (DMEM, Gibco, Carlsbad, CA, USA), 10% Fetal Bovine Serum (FBS, Gibco, Carlsbad, CA, USA), and 1% penicillin–streptomycin (100 \times) (Gibco, Carlsbad, CA, USA). Cell viability at different selenadiazole treatment levels was assessed using the Cell Count Kit-8 (CCK-8, Beyotime, Shanghai, China). Initially, cells were dissociated using 0.25%

Trypsin-EDTA (Gibco, Carlsbad, CA, USA) and seeded at a density of 10^5 cells per $1000 \mu\text{L}$ in a 96-well plate.

Detection of Mitochondrial Membrane Potential ($\Delta\Psi\text{m}$). The decrease in mitochondrial membrane potential is one of the tokens of apoptosis, which could be detected by the JC-1 fluorescence probe (Beyotime, Shanghai, China). HeLa cells were seeded in a 6-well plate with selenadiazole

diluted by a complete culture medium for 24 h. First, the medium was removed, and PBS was utilized for washing. Then, we added 2000 μL of JC-1 staining reagent into each well and put them into a 37 °C, 5% CO₂ incubator. Twenty minutes later, the JC-1 staining reagent was obsolete, and we added JC-1 buffer into each well to clear away the extra JC-1 staining reagent. Ultimately, we put a complete culture medium into each well and observed the distribution of JC-1 monomers and aggregates using a fluorescence microscope. For the quantitative experiment, we first digested cells into a suspension and then repeated the steps mentioned above. Flow cytometry was applied for detecting fluorescence and a quantitative analysis.

AnnexinV-PI Double Staining Assay. An AnnexinV-FITC Apoptosis Detection Kit was purchased from Beyotime (Shanghai, China). HeLa cells were seeded in a 6-well plate with selenadiazole diluted by a complete culture medium for 24 h. First, the medium was removed and collected in 15 mL centrifuge tubes, and HeLa cells were placed into a state of suspension. Then, the cells were centrifuged and collected. We added 195 μL of AnnexinV staining reagent and 10 μL of propidium iodide (PI) staining reagent into each centrifuge tube and placed them at room temperature away from moisture and light for 15 min. Finally, flow cytometry was applied for detecting fluorescence and quantitative analysis. For qualitative analysis, we prepared HeLa cells for *in situ* staining and grabbed the morphological features from a fluorescence microscope.

Detection of Redox Oxygen Species. HeLa cells were seeded in a 6-well plate with selenadiazole diluted by a complete culture medium for 24 h. First, the medium was removed, and PBS was utilized for washing. Then, we added 1000 μL of DCFH-DA probe reagent into each well and put them into a 37 °C, 5% CO₂ incubator. Twenty minutes later, we used a DMEM medium to clear away extra DCFH-DA. Finally, we observe the distribution of ROS through a fluorescence microscope. For the quantitative experiment, we first digested cells into a state of suspension and then repeated the steps mentioned above. We detected the ROS levels through an ELIASA machine (ThermoFisher, Waltham, Massachusetts, USA).

Detection of Caspase-3 and Caspase-9. HeLa cells were seeded in 6 cm culture dishes with selenadiazole diluted by a complete culture medium for 24 h. We used trypsin to collect cells and added PBS to clear away the extra complete culture medium. Then, we obsolete the liquid supernatant and put cell lysate into each centrifuge tube on ice. After 30 min, we put them at 15,000 rpm, 30 min, 4 °C centrifuge machine (Eppendorf, Hamburg, Germany). We took the liquid supernatant and mixed it into a caspase reaction system (including sample, buffer, trypsin, Ac-LEHD-pNA for caspase-9, and Ac-DEHD-pNA for caspase-3) in a 96-well plate. After waiting for 8 h, we detected the absorbance value in 405 nm and adjusted their caspase concentration by the total protein concentration that was examined by a Bradford Assay Kit (Beyotime, Shanghai, China).

Western Blotting. We added our combined lysate (RIPA, PMSF, and phosphatase inhibitors included; Beyotime, Shanghai, China) into cells. A BCA Protein Assay Kit (Beyotime, Shanghai, China) was utilized for adjusting the loading volume of the protein sample. For electrophoresis, we used a 10% PAGE Gel Fast Preparation Kit (Epizyme, Shanghai, China) and finished the process in a condition of

120 V, 40 min. When it came to transferring, we used PVDF membrane (Millipore, Darmstadt, Germany) and stayed at a condition of 90 V, for 100 min. Then, we put the PVDF membrane into a protein-free blocking buffer (Solarbio, Beijing, China). We incubated the PVDF membrane with primary antibodies (Cellsignaling Technology, Boston, USA) for 12 h in a 4 °C shaker. After that, the PVDF membrane was covered with secondary antibodies (Cellsignaling Technology, Boston, USA). Ultimately, a Chemistar High-sig ECL Western Blotting Substrate (Tanon, Shanghai, China) was used for imaging the protein.

Statistical Analysis. Statistical analysis was conducted in GraphPad (San Diego, California, USA). Continuous variants are represented as mean \pm SD *t* test and a one-way or two-way analysis of variants were utilized.

AUTHOR INFORMATION

Corresponding Authors

Jinying Yang – Department of Obstetrics, Longgang District Maternity and Child Healthcare Hospital of Shenzhen City (Longgang Maternity and Child Clinical Institute of Shantou University Medical College), Shenzhen 510080, China; Email: yangjinying1981@126.com

Jing Zhang – Department of Interventional Radiology, Guangdong Provincial People's Hospital (Guangdong Academy of Medical Sciences), Southern Medical University, Guangzhou, Guangdong 510080, China; Email: zhangjing2846@gdph.org.cn

Authors

Yi Yuan – Center Laboratory, Guangzhou Women and Children's Medical Center, Guangzhou Medical University, Guangzhou 510120, China

Yinghua Li – Center Laboratory, Guangzhou Women and Children's Medical Center, Guangzhou Medical University, Guangzhou 510120, China; orcid.org/0009-0006-5463-2849

Qinglin Deng – Nanfang Hospital, Southern Medical University, Guangzhou 510120, China

Complete contact information is available at:

<https://pubs.acs.org/10.1021/acsomega.3c10107>

Author Contributions

[†]Y.Y. and Y.L. contributed equally to this work. Y.Y. designed the study, carried out the experiments, and drafted the manuscript. Y.L. analyzed the experimental data. Q.D. drafted the manuscript. J.Y. and J.Z. refined the manuscript and coordinated the study. All authors read and approved the final manuscript.

Notes

The authors declare no competing financial interest.

ACKNOWLEDGMENTS

This work was supported by the technology planning projects of Guangzhou (202201020655) and the Guangdong Natural Science Foundation (2020A1515110648).

ABBREVIATIONS

CCK-8, cell count kit-8; ROS, redox oxygen species; HR-HPV, high-risk human papillomavirus; Se, selenium; PARP, poly ADP-ribose polymerase; ATCC, American Type Culture Collection; DMEM, Dulbecco's modified Eagle medium;

FBS, Fetal Bovine Serum; PI, propidium iodide; PB, phosphate buffered saline

REFERENCES

- (1) Sung, H.; Ferlay, J.; Siegel, R. L.; Laversanne, M.; Soerjomataram, I.; Jemal, A.; Bray, F. Global Cancer Statistics 2020: GLOBOCAN Estimates of Incidence and Mortality Worldwide for 36 Cancers in 185 Countries. *CA A Cancer J. Clinicians* **2021**, *71* (3), 209–249.
- (2) Aswathy, S.; Reshma, J.; Avani, D. Epidemiology of Cervical Cancer with Special Focus on India. *Int. J. Womens Health* **2015**, *7*, 405–414.
- (3) Guo, C.; Qu, X.; Tang, X.; Song, Y.; Wang, J.; Hua, K.; Qiu, J. Spatiotemporally Deciphering the Mysterious Mechanism of Persistent HPV-Induced Malignant Transition and Immune Remodelling from HPV-Infected Normal Cervix, Precancer to Cervical Cancer: Integrating Single-Cell RNA-Sequencing and Spatial Transcriptome. *Clin Transl Med.* **2023**, *13* (3), No. e1219.
- (4) Wei, E.; Reisinger, A.; Li, J.; French, L. E.; Clanner-Engelshofen, B.; Reinholz, M. Integration of scRNA-Seq and TCGA RNA-Seq to Analyze the Heterogeneity of HPV+ and HPV- Cervical Cancer Immune Cells and Establish Molecular Risk Models. *Front Oncol* **2022**, *12*, No. 860900.
- (5) Sosa, V.; Moliné, T.; Somoza, R.; Paciucci, R.; Kondoh, H.; LLeonart, M. E. Oxidative Stress and Cancer: An Overview. *Ageing Res. Rev.* **2013**, *12* (1), 376–390.
- (6) Srinivas, U. S.; Tan, B. W. Q.; Vellayappan, B. A.; Jeyasekharan, A. D. ROS and the DNA Damage Response in Cancer. *Redox Biol.* **2019**, *25*, No. 101084.
- (7) Cheung, E. C.; Vousden, K. H. The Role of ROS in Tumour Development and Progression. *Nat. Rev. Cancer* **2022**, *22* (5), 280–297.
- (8) Kang, D.; Lee, J.; Jung, J.; Carlson, B. A.; Chang, M. J.; Chang, C. B.; Kang, S.-B.; Lee, B. C.; Gladyshev, V. N.; Hatfield, D. L.; Lee, B. J.; Kim, J.-H. Selenophosphate Synthetase 1 Deficiency Exacerbates Osteoarthritis by Dysregulating Redox Homeostasis. *Nat. Commun.* **2022**, *13* (1), 779.
- (9) Lai, H.; Xu, L.; Liu, C.; Shi, S.; Jiang, Y.; Yu, Y.; Deng, B.; Chen, T. Universal Selenium Nanoadjuvant with Immunopotentiating and Redox-Shaping Activities Inducing High-Quality Immunity for SARS-CoV-2 Vaccine. *Sig Transduct Target Ther* **2023**, *8* (1), 88.
- (10) Jia, Y.; Li, G.; Wang, R.; Feng, C.; Qi, L.; Wang, Y.; Su, S.; Zou, Y.; Liu, X.; Wang, Y.; Zhang, Y.; Du, L.; Sun, H.; Hao, S.; Hou, J.; Feng, H.; Li, Q.; Wang, T. A County-Level Spatial Epidemiological Study of Hair Selenium and Keshan Disease. *Front Nutr* **2022**, *9*, 1011460.
- (11) Yuan, S.; Mason, A. M.; Carter, P.; Vithayathil, M.; Kar, S.; Burgess, S.; Larsson, S. C. Selenium and Cancer Risk: Wide-Angled Mendelian Randomization Analysis. *Int. J. Cancer* **2022**, *150* (7), 1134–1140.
- (12) Mojadadi, A.; Au, A.; Salah, W.; Witting, P.; Ahmad, G. Role for Selenium in Metabolic Homeostasis and Human Reproduction. *Nutrients* **2021**, *13* (9), 3256.
- (13) Liu, C.; Lin, R.; Lai, H.; Pi, F.; Xue, Q.; Chen, T.; He, W. Thermosensitive Selenium Hydrogel Boosts Antitumor Immune Response for Hepatocellular Carcinoma Chemoradiotherapy. *Nano Today* **2023**, *50*, No. 101823.
- (14) Chen, M.; Cao, W.; Wang, J.; Cai, F.; Zhu, L.; Ma, L.; Chen, T. Selenium Atom-Polarization Effect Determines TrxR-Specific Recognition of Metallo drugs. *J. Am. Chem. Soc.* **2022**, *144* (45), 20825–20833.
- (15) Chen, T.; Zheng, W.; Wong, Y.-S.; Yang, F. Mitochondria-Mediated Apoptosis in Human Breast Carcinoma MCF-7 Cells Induced by a Novel Selenadiazole Derivative. *Biomed Pharmacother* **2008**, *62* (2), 77–84.
- (16) Xie, Q.; Zhou, Y.; Lan, G.; Yang, L.; Zheng, W.; Liang, Y.; Chen, T. Sensitization of Cancer Cells to Radiation by Selenadiazole Derivatives by Regulation of ROS-Mediated DNA Damage and ERK and AKT Pathways. *Biochem. Biophys. Res. Commun.* **2014**, *449* (1), 88–93.
- (17) Liu, X.; Lai, J.; Su, J.; Zhang, K.; Li, J.; Li, C.; Ning, Z.; Wang, C.; Zhu, B.; Li, Y.; Zhao, M. Selenadiazole Inhibited Adenovirus-Induced Apoptosis through the Oxidative-Damage-Mediated Bcl-2/Stat 3/NF- κ B Signaling Pathway. *Pharmaceuticals (Basel)* **2023**, *16* (10), 1474.
- (18) Xie, Q.; Li, Z.; Luo, X.; Wang, D.; Zhou, Y.; Zhao, J.; Gao, S.; Yang, Y.; Fu, W.; Kong, L.; Sun, T. piRNA-14633 Promotes Cervical Cancer Cell Malignancy in a METTL14-Dependent m6A RNA Methylation Manner. *J. Transl Med.* **2022**, *20* (1), 51.
- (19) Abbas, Y.; Turco, M. Y.; Burton, G. J.; Moffett, A. Investigation of Human Trophoblast Invasion in Vitro. *Hum Reprod Update* **2020**, *26* (4), 501–513.
- (20) Elefantova, K.; Lakatos, B.; Kubickova, J.; Sulova, Z.; Breier, A. Detection of the Mitochondrial Membrane Potential by the Cationic Dye JC-1 in L1210 Cells with Massive Overexpression of the Plasma Membrane ABCB1 Drug Transporter. *Int. J. Mol. Sci.* **2018**, *19* (7), 1985.
- (21) Poltorak, A. Cell Death: All Roads Lead to Mitochondria. *Curr. Biol.* **2022**, *32* (16), R891–R894.
- (22) Lindsay, J.; Esposti, M. D.; Gilmore, A. P. Bcl-2 Proteins and Mitochondria—Specificity in Membrane Targeting for Death. *Biochim. Biophys. Acta* **2011**, *1813* (4), 532–539.
- (23) Cui, L.; Bu, W.; Song, J.; Feng, L.; Xu, T.; Liu, D.; Ding, W.; Wang, J.; Li, C.; Ma, B.; Luo, Y.; Jiang, Z.; Wang, C.; Chen, J.; Hou, J.; Yan, H.; Yang, L.; Jia, X. Apoptosis Induction by Alantolactone in Breast Cancer MDA-MB-231 Cells through Reactive Oxygen Species-Mediated Mitochondrion-Dependent Pathway. *Arch Pharm. Res.* **2018**, *41* (3), 299–313.
- (24) Green, D. R. The Mitochondrial Pathway of Apoptosis Part II: The BCL-2 Protein Family. *Cold Spring Harb. Perspect. Biol.* **2022**, *14* (6), No. a041046, DOI: 10.1101/cshperspect.a041046.
- (25) Eskandari, E.; Eaves, C. J. Paradoxical Roles of Caspase-3 in Regulating Cell Survival, Proliferation, and Tumorigenesis. *J. Cell Biol.* **2022**, *221* (6), No. e202201159, DOI: 10.1083/jcb.202201159.
- (26) Liu, J.; Wu, F.; Wang, M.; Tao, M.; Liu, Z.; Hai, Z. Caspase-3-Responsive Fluorescent/Photoacoustic Imaging of Tumor Apoptosis. *Anal. Chem.* **2023**, *95* (25), 9404–9408.
- (27) Sánchez-de-Diego, C.; Valer, J. A.; Pimenta-Lopes, C.; Rosa, J. L.; Ventura, F. Interplay between BMPs and Reactive Oxygen Species in Cell Signaling and Pathology. *Biomolecules* **2019**, *9* (10), 534.
- (28) Diwanji, N.; Bergmann, A. An Unexpected Friend - ROS in Apoptosis-Induced Compensatory Proliferation: Implications for Regeneration and Cancer. *Semin Cell Dev Biol.* **2018**, *80*, 74–82.
- (29) Morgan, E. L.; Macdonald, A. JAK2 Inhibition Impairs Proliferation and Sensitises Cervical Cancer Cells to Cisplatin-Induced Cell Death. *Cancers (Basel)* **2019**, *11* (12), 1934.
- (30) Ran, S.; Ren, Q.; Li, S. JAK2/STAT3 in Role of Arsenic-Induced Cell Proliferation: A Systematic Review and Meta-Analysis. *Rev. Environ. Health* **2022**, *37* (3), 451–461.
- (31) Wang, X.; Dai, C.; Yin, Y.; Wu, L.; Jin, W.; Fu, Y.; Chen, Z.; Hao, K.; Lu, B. Blocking the JAK2/STAT3 and ERK Pathways Suppresses the Proliferation of Gastrointestinal Cancers by Inducing Apoptosis. *J. Zhejiang Univ Sci. B* **2021**, *22* (6), 492–503.
- (32) Leonard, W. J.; O'Shea, J. J. Jaks and STATs: Biological Implications. *Annu. Rev. Immunol.* **1998**, *16*, 293–322.
- (33) Darnell, J. E. J. STATs and Gene Regulation. *Science* **1997**, *277* (5332), 1630–1635.
- (34) Mengie Ayele, T.; Tilahun Muche, Z.; Behaile Teklemariam, A.; Bogale, A.; Chekol Abebe, E. Role of JAK2/STAT3 Signaling Pathway in the Tumorigenesis, Chemotherapy Resistance, and Treatment of Solid Tumors: A Systemic Review. *J. Inflammable Res.* **2022**, *15*, 1349–1364.